QUARK FRAGMENTATION IN $e^+ e^-$ COLLISIONS *

P. Oddone
Lawrence Berkeley Laboratory
University of California
Berkeley, CA 94720

OUTLINE

I. INTRODUCTION AND COMMENT ON MODELS

II. PARTICLE PRODUCTION

Stable particles: π, K, p, Λ, Ξ, and resonances: ρ, ϕ, K^*.

III. PARTICLES IN EVENTS

a) Rapidity distributions relative to the event axis,

b) $p_\perp$ distributions relative to the event axis,

c) Three jet events: properties of the gluon jet (more baryons?),

particle flow as a function of particle type, energy-energy correlation.

IV. PARTICLE CORRELATIONS

a) Flavor correlations,

b) Baryon-baryon correlations.

V. CONCLUSION

---

* This work was supported by the U.S. Department of Energy under Contract Number DE-AC03-76SF00098

© P. Oddone

I. INTRODUCTION AND A COMMENT ON MODELS

In this brief review of new results in quark and gluon fragmentation observed in $e^+ e^-$ collisions, I have been quite selective; I shall concentrate mostly on PEP results and, within PEP, mostly on TPC results. The new PETRA results have been reported at this conference by M. Davier.[1] Given the organization of the topical conference I have restricted myself to results on light quark fragmentation since the results on heavy quark fragmentation have been reported by J. Chapman.[2]

In the study of fragmentation we try to understand how a state of initial partons at large Q^2 and small distances evolves in time and finally manifests itself in the laboratory as the usual mesons and baryons. We believe that quantum chromodynamics of quasi-free quarks and gluons is the correct dynamical description of the initial stages of the process.[3] The remnant of this few parton stage is observed in the laboratory as jets, ensembles of particles in which each particle has a small transverse momentum relative to the sum of momenta of the particles in the ensemble. While the initial observation of jets at SPEAR[4] was based on the statistical study of many events, jets observed at PEP and PETRA are dramatic and clear on an event by event basis. The first observation of hard gluon radiation as three jet events at PETRA[5] was conclusive after a handful of events. It is precisely the distinct nature of jets which makes the study of fragmentation interesting: to the extent the jets "remember" the original parton momentum they provide a means to test QCD calculations of the initial few parton stage; conversely, as we gain confidence in QCD calculations we can begin to explore models which evolve this initial state into the finally observed hadrons. The confinement mechanism which prevents the existence of free quarks and gluons is not a well understood process. It is the inability to make rigorous calculations and predictions which has led to the creation of several phenomenological models which attempt to describe the data with relatively few parameters. Thus in the following paragraphs we compare the data with three phenomenological models: the independent fragmentation model (IF),[6] the Lund string model (LUND)[7] and the QCD cascade models of Webber[8] and Gottschalk.[9] These models are constantly evolving and have variants in the treatment of specific subprocesses (e.g. baryon formation). Thus LUND has evolved from "early LUND" to "standard LUND" to "symmetric LUND," the IF model has five or more variants depending on how the gluon is treated and how one implements energy and momentum conservation, and the QCD cluster models differ on how far the quark-gluon cascade is evolved before the formation of colorless clusters and on how the decay of clusters is matched to the existing data. With such multiplicity of models it becomes difficult to make definitive statements as to when such models fail in a fundamental way as opposed to failures which can be "fixed" without doing violence to the principles of the model. It is indeed a sign of progress that the new data allows us to make definitive statements regarding the failure of some models. The new data also provides a much higher level of detail which the models will have to attempt to fit or "explain."

Table I shows schematically some of the principal parameters of the models for the three families of models mentioned above. Typical parameters for the IF and LUND models are fragmentation functions, flavor suppression factors for the production of quark pairs, vector to pseudoscalar ratio for particle production, and additional parameters to describe baryon production which is handled in a variety of prescriptions. For the QCD cascade or cluster models the parameters are the QCD scale Λ, cut-off parameters for gluon radiation, mass parameters

As examples of the progress made during last year I have selected some of the measurements and will describe them in brief detail. One interesting new measurement has been made by the HRS[11] using its superb momentum resolution ($dp/p^2 \simeq 0.1\%$, p in GeV) in the region $x = z \rightarrow 1$, where $x = 2E_h/\sqrt{s}$ and s is the total center of mass energy. Here they have looked for the presence of a constant term in the differential cross section for charged particle production as expected by some models.[12] The differential cross section is shown in Figure 1. In the region of large x they find:

$$F(x) \propto (1-x)^2 + \mu^2/Q^2$$

where the 90% CL is $\mu < 4.4$ GeV/c.

Figure 2 illustrates the rapid progress in the measurement of ϕ production from the first measurements by TPC reported last summer[13] to the measurements reported by HRS this summer.[14] The LUND model prediction for ϕ production is also shown in the figure, and shows good agreement with the data.

Figure 3 illustrates the typically good agreement which the various experiments show when they measure the same process. The figure shows the differential cross section for Λ production as measured by MkII,[15] TASSO,[16] JADE[17] and TPC.[18] The LUND model prediction is shown superimposed on the data.

Figure 4 shows the differential cross section for K^+/K^-, $K^0/\bar{K}^0$, $K^{*0}/\bar{K}^{*0}$, and ϕ as measured by the TPC[19] together with the LUND model predictions. The cross sections for K^{*0} are not well reproduced by the present model

TABLE II: LIGHT MESON YIELD @ 29 --->34 GEV

Particle	MKII	TPC	HRS	DELCO	TASSO	JADE
ρ^o	★22 0.41 ±0.07 p>1 GeV		★33 0.58 ±0.06 x>.1		20 0.41 0.08 .1<x<.7	★24 0.98 ±0.17
K^{*o}	★22 0.35 ±0.09 p>1 GeV	★19 0.49 ±0.09	★33 0.36 ±0.06 x>.1	★25 large momenta		
$K^{*\pm}$	★22 0.29 ±0.10 p>2 GeV		★33 0.31 ±0.11 x>.1			★24 0.87 ±0.18
ϕ		★13 0.08 ±0.02	★14 0.08 ±0.01	★25 large momenta		
$K^{\pm}$	★26 small x only	★21 1.35 ±0.13			27 2.0 ±0.2	
K^o	★22 1.22 ±0.14	★19 1.22 ±0.15	★23 1.40 ±0.12		★28 1.60 ±0.1	★29 1.45 ±0.17
$\pi^{\pm}$		★21 10.7 ±0.6			27 10.3 ±0.4	
π^o		★30 5.3 ±0.6			31 6.1 ±2.0	
η						32 0.76 ±0.28

★≡NEW MEASUREMENT IN LAST YEAR. nn ≡REFERENCE NUMBER
SEE EXPLANATION OF NOMENCLATURE IN THE CAPTION OF TABLE III.

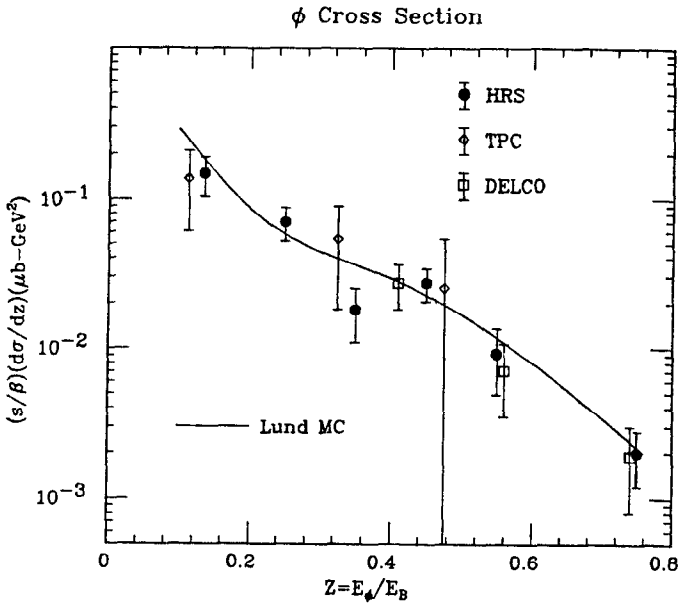

FIGURE 2

The ϕ inclusive differential cross section as a function of $z = E_\phi/E_{beam}$ as measured by the HRS, TPC and DELCO collaborations. See text for references.

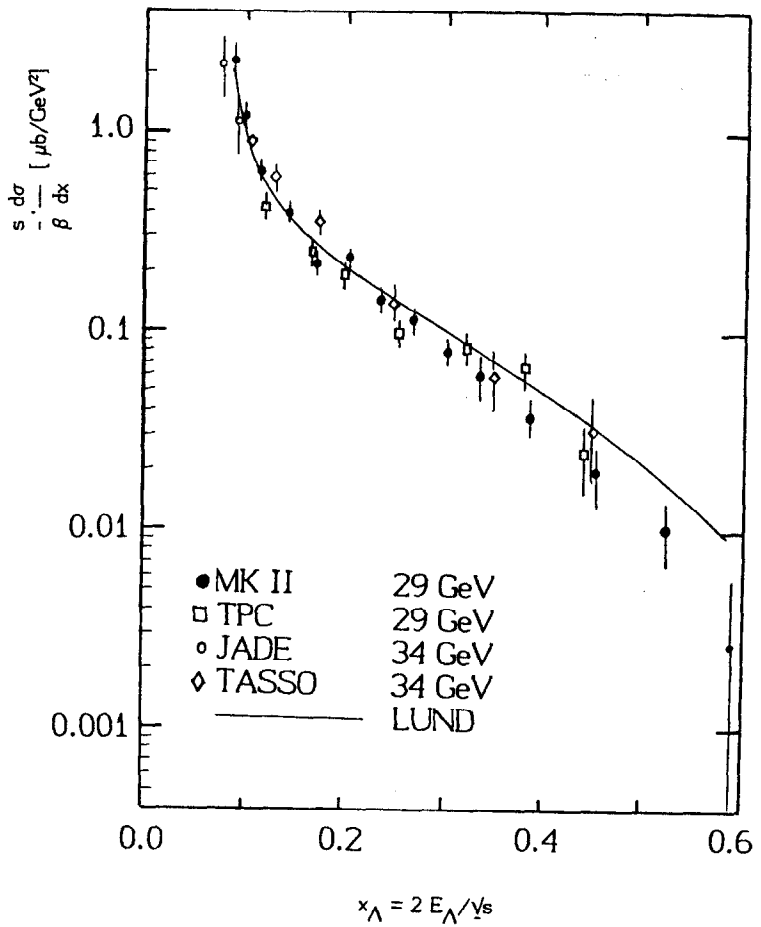

FIGURE 3

Inclusive Λ production as a function of $x = 2E_\Lambda/\sqrt{s}$ measured by the TPC, MKII, JADE and TASSO collaborations. See text for references.

$$n_c(K^{\pm}) = 0.86 \pm 0.15.$$

With the further assumption that the number of $K^{\pm *}$ is equal to K^{o*} we derive a ratio V/(V+P)= 0.48 ± 0.15. This example illustrates that even after the measurement of particle production a considerable amount of gymnastics is involved in deriving a model parameter such as V/(V+P). The error in the parameter depends on statistics and systematic errors of several measurements and on uncertainties in the decay branching ratios of charm and bottom resonances.

As a further example we can use the measured production fractions of ϕ's and K^{o*} to estimate the suppression factor for the production of $s\bar{s}$ pairs out of the vacuum. This ratio is

$$s/u = 2N(\phi)/N(K^{o*}) = 0.37 \pm 0.15 \pm 0.8$$

after correction for charm and bottom decay. Using the measurement of ρ^o from TASSO[20] we further obtain

$$s/u = N(K^{o*})/2N(\rho^o) = 0.32 \pm 0.09 \pm 0.05$$

indicating that a single parameter s/u appears to govern the ϕ/K^{o*} and the K^{o*}/ρ^o production ratios as is assumed in many fragmentation models.

Much work remains to be done to obtain the best parametrization of the various models. Many distributions are now becoming available, not only for single particles but, as we shall see further on, for particle distributions in relation to global event properties and in relation to other particles. We are beginning to do global fits to all available distributions. This work is in its early stages and no definitive numbers are yet available.

PARTICLES IN EVENTS

New data is now available on the production properties of different particles in relation to the event axis. These data are generally presented as rapidity distributions relative to the event axis and as transverse momentum distributions relative to the event axis. In addition it is possible to study particle production in events with three jets and thus be sensitive to differences between gluon and quark jets. In what follows we generally use the sphericity axis as the event axis unless explicitly stated otherwise.

A. Rapidity Distributions

TASSO[35] has studied rapidity distributions as a function of energy. As expected, with the standard definition of rapidity

$$y = 1/2 \ln \frac{E + p_L}{E - p_L},$$

the rapidity distributions show a plateau which broadens as a function of the energy. In addition a very shallow dip near zero rapidities was observed. New information is now available with separation of the different particle species π's, K's and p's. In particular, the small dip in the rapidity plateau near zero rapidity can be investigated as a function of particle type. This study is interesting because different models predict different behaviour near zero

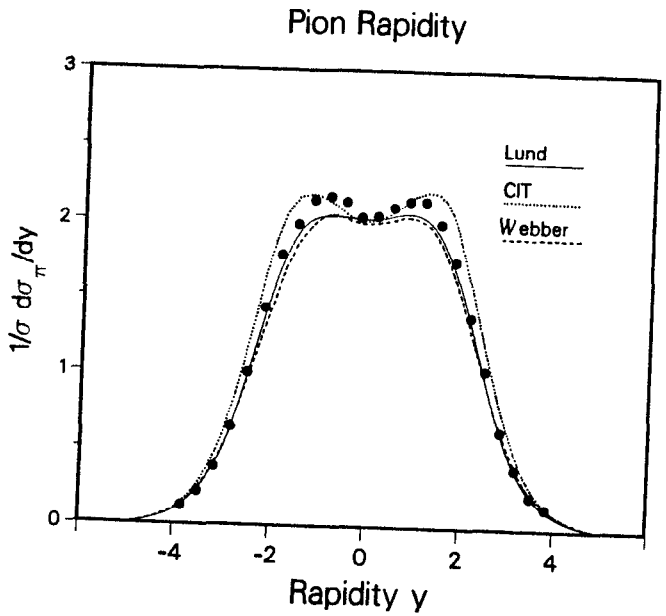

FIGURE 6

Pion inclusive rapidity distribution for identified pions measured by the TPC.

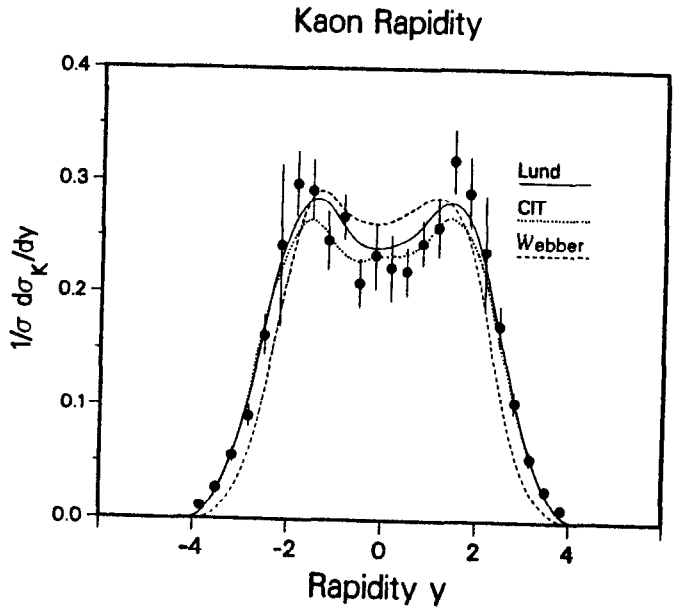

FIGURE 7

Kaon inclusive rapidity distribution for identified kaons measured by the TPC.

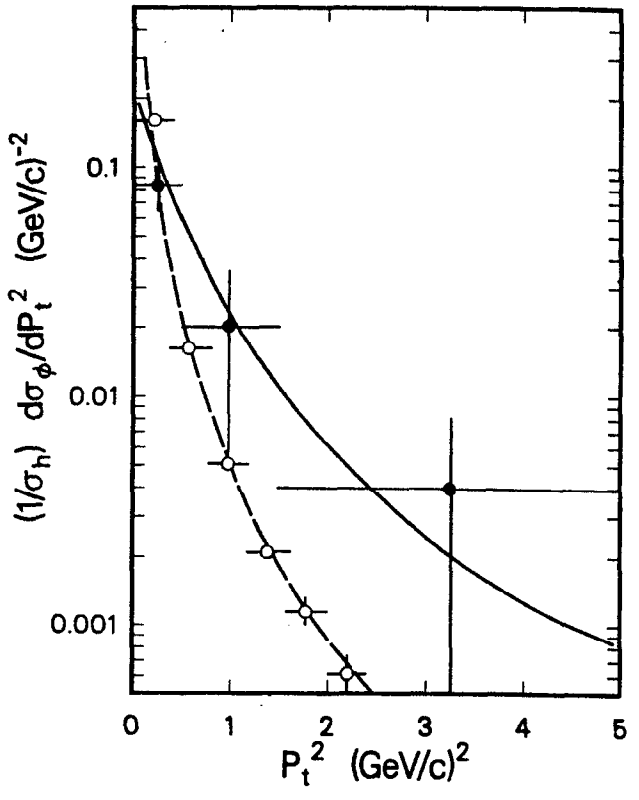

FIGURE 9

Distribution of the square of the ϕ transverse momentum with respect to the thrust axis in the range $x_\phi < 0.55$ (indicated by filled circles). The open circles give the distribution observed for $\pi^\pm$ scaled by 1/140. The solid and dashed lines show the predictions of the LUND model. The data is from the TPC.

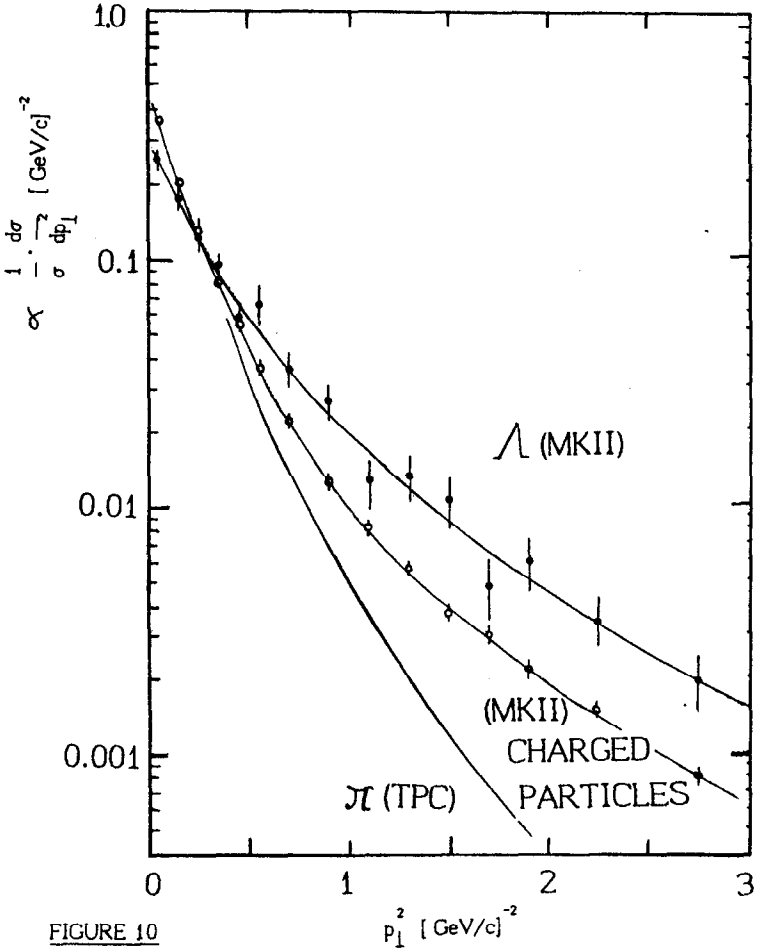

FIGURE 10

Transverse momentum distribution relative to the thrust axis for Λ's (upper curve) and all charged particles (middle curve), both measured by the MKII, compared to π's measured by the TPC (lower curve).

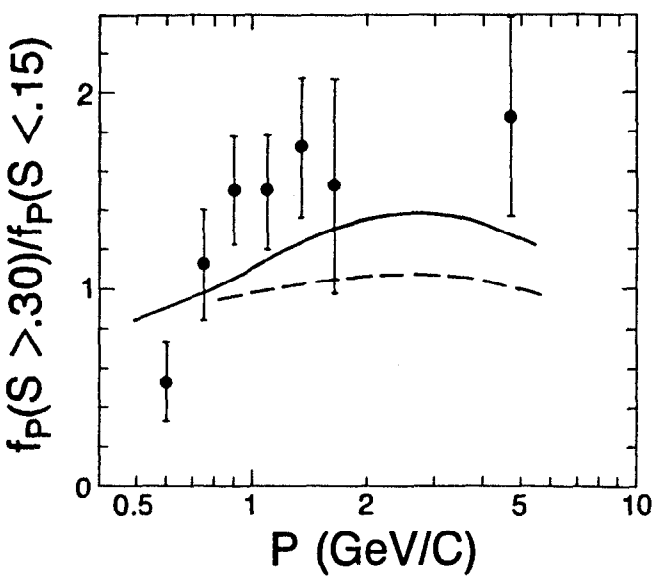

FIGURE 12

The ratio of proton fractions in events with high (>.3) and low (<.15) sphericity, as a function of momentum. Full and dashed lines show the predictions of the LUND model for final state hadrons and primary hadrons respectively. The data is from the TPC.

present in two jet events. Furthermore, the ratio of primary baryon production for events of high and low sphericity is approximately flat and equal to 1 in the model. The enhanced proton production predicted by the model exists only after resonance decay as is shown by the solid line in Figure 12. Thus purely kinematical effects are able to account for the enhanced proton production without invoking a different mechanism for proton production in gluon fragmentation.

Particle flow in three jet events: A test of models

One important question which differentiates models is whether or not the observed hadrons originate from sources which are Lorentz-boosted relative to the overall center of mass system. JADE[37,38] has reported that particle flow in three jet events favors the LUND model over the IF model. TPC has now confirmed this effect and extended the study to additional models,[39,40] using better particle identification.

In IF models, each parton fragments into a jet of hadrons independently. Thus in three jet events the regions between the jets are populated by the same mechanism: the momentum distribution transverse to the jet axes (Figure 13a).

In the LUND model three jet events are represented by a string that stretches from the quark to the gluon and then to the antiquark (Figure 13b). The two string segments fragment in their respective rest frames. Hadrons thus receive a Lorentz boost as observed in the overall center of mass system. As a result the distribution of hadrons in the regions between the jets is altered: the region qg and the region $\bar{q}g$ are favored by the boost, while the region $q\bar{q}$ is comparatively

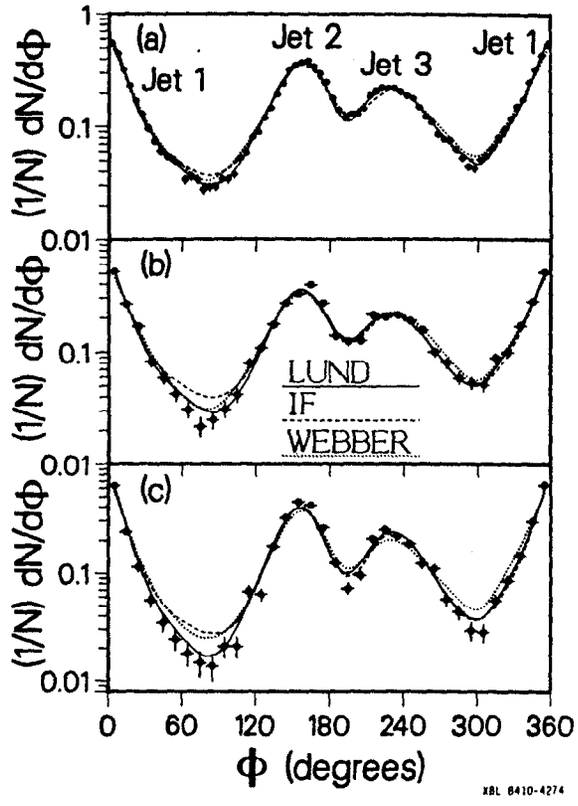

FIGURE 14

Particle density $(1/N)dN/d\phi$ in 3-jet events for (a) all charged particles and photons, (b) those charged particles and photons satisfying $0.3 < p_{out} < 0.5$ GeV, where p_{out} is the momentum out of the event plane, and (c) a heavy particle sample of charged and neutral K's, p's and Λ's. Also shown are the predictions of the IF, LUND and Webber cluster models. The data is from the TPC.

where it predicts a density 30% higher than the data. As expected from the nature of the Lorentz boost, the effects are accentuated for particles with large transverse mass $m_\perp = \sqrt{m^2 + p_\perp^2}$. Thus the discrepancy with the IF model increases to a factor of 2 for either particles with large momentum relative to the event plane or for particles with large mass. The discrepancy is fundamental and cannot be "patched-up" in the present variants of the IF model: the IF model cannot be tuned to fit the 1-2 valley and provide reasonable fits of global event distributions. For the Webber model the predictions are too large for all regions between jets; this result is sensitive to model parameters which have not been tuned for this particular analysis.

A quantitative summary can be made by studying the "normalized particle populations " N_{ij}. For each particle between jets i and j the angle between the jet i and the particle is divided by the angle between jets i and j; N_{ij} is the number of particles between .3 and .7 in this normalized angular region (the most sensitive to boost effects). The comparison of the jet 1-2 region and the jet 1-3 region is made by the ratio N_{31}/N_{12}. This ratio is insensitive to the variants of the IF model, to tuning of the Webber model and to detector acceptance. For IF models we expect $N_{31}/N_{12} \simeq 1$ independent of particle mass or transverse momentum out of the plane, while for boosted hadron sources in the LUND and Webber models we expect the ratio to be greater than 1 and to increase with mass and momentum out of the plane.

The ratio N_{31}/N_{12} is shown in Figure 15. The data show that the ratio increases with mass and with momentum out of the plane. The LUND and the Webber models give a good description of the behaviour of this ratio, while the IF model does not fit the data.

numbers. On the other hand, the final formation of hadrons is a small Q^2 phenomenon which we expect will generate short range correlations (SRC's). Figure 16 illustrates the mechanisms for LRC's and SRC's in the case of (a) pions arising from primary light quarks and (b) pions and kaons arising from heavy quarks.

With the usual definition of rapidity (see discussion of rapidity distributions above) we can define the flavor tagged charge density $q_a^b(y)$ as the net compensating charge density seen in particles of species b when the test particle is of species a:

$$q_a^b(y) = \rho_b^{opposite\ a}(y) - \rho_b^{same\ a}(y)$$

where the superscripts *opposite* (*same*) a indicate particles of species b with the opposite (same) charge as a. When calculating $q_a^b(y)$ the data must be corrected for sample purity and detection efficiency by unfolding the measured two particle π, K and p combinations using Monte Carlo determined misidentification probabilities and acceptances.

Figures 17a and 17b show the $\pi\pi$ rapidity correlations with results similar to the charge compensation results previously observed in e^+e^-[43] and pp[44] collisions. When the test π is chosen at small rapidity y_{test} the dominant feature is SRC's due to resonance decay and presumably local charge compensation in the hadronization process. For large y_{test} LRC's become evident and provide evidence for charged primary partons.

Figure 18a shows KK correlations for large y_{test}. The LRC is now

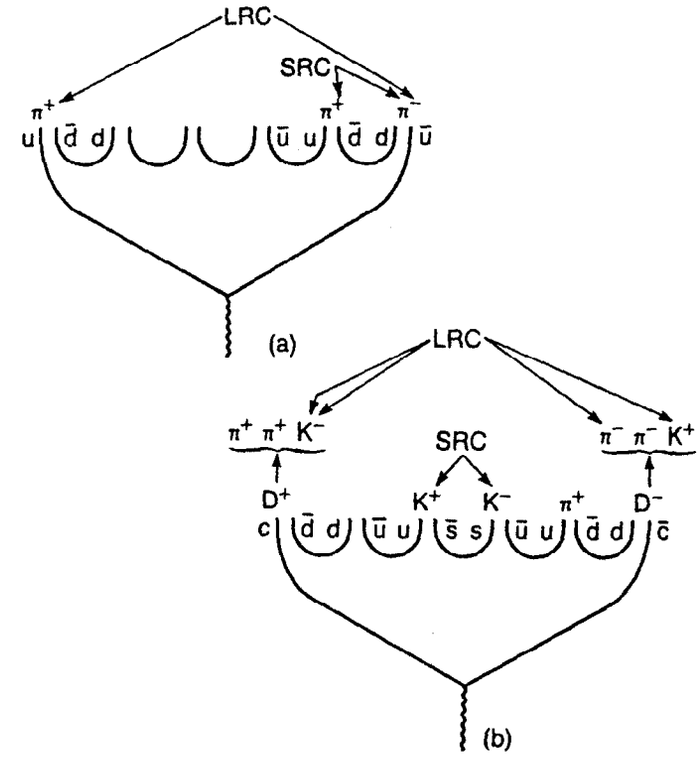

FIGURE 16

The mechanisms responsible for long- and short-range flavor correlations (a) among pions and (b) between pions and kaons.

comparable in size to the SRC and large in contrast to the $\pi\pi$ case in which the LRC was a factor of six smaller than the SRC. Unlike the $\pi\pi$ case, the decay of resonances is expected to be a small contribution to the SRC. For small y_{test} the ϕ is expected to contribute about 10% of the SRC, and it should be the only contribution if primary mesons are produced in the ground state scalar and vector nonets. For large y_{test}, the ϕ contributes about 15% and the $F \rightarrow \phi\pi$ contributes about 5% of the SRC. It appears, therefore, that the KK SRC cannot be explained by resonance decay and is evidence of soft hadronization with local compensation of flavor. The relatively large LRC shown in the figure indicates that for this y_{test} a large fraction of the K's are direct descendants from primary heavy quarks.

Figure 18b shows the size of the πK correlation to be much smaller than either the $\pi\pi$ or the KK correlations. The observed SRC is due to a combination of local charge conservation during hadronization and decays such as $K^{*o} \rightarrow K^{+}\pi^{-}$. It is interesting to note that the LRC is of opposite sign than the KK LRC as is expected from the decay of primary charm particles (see Figure 16).

The curves superimposed on Figures 17 and 18 correspond to the LUND model (solid line), the Webber QCD cluster model (dotted line) and the LUND model without heavy (b and c) quarks (dashed line). The latter model is included to show explicitly the SRC's and LRC's introduced by heavy quark decays. In general both the LUND and the Webber models represent the features of the data quite well. The small existing disagreements are not known to be fundamental at this time.

The global conclusions from these correlations studies are: short range

correlations exist and support the hypothesis that quantum numbers are locally conserved during the hadronization process, and long range correlations provide evidence that jets are produced by flavor carrying quarks. Furthermore the detailed information now available provides additional constraints on models.

B. Baryon-baryon correlation

While the production of quark-antiquark pairs out of the vacuum is a natural feature of most models, the production of three-quark color singlet states as required for baryon formation is often an ad-hoc feature of the models. Even to test whether baryon pairs are produced close by in rapidity space, i.e. compensate baryon number locally, or are produced more or less randomly in rapidity space, i.e. conserve baryon number globally, is a difficult experimental question. Baryons are less common, and the efficiency for identifying them is usually low. Data is now becoming available on baryon-baryon correlations, albeit with relatively low statistics. TASSO[45] has reported data on pp and $p\bar{p}$ correlations at baryon momenta in the 1 to 5GeV/c range showing evidence for local baryon compensation. TPC[46] with a considerably larger number of $p\bar{p}$ events (179) at momenta below 1.5 GeV/c also favors local baryon number conservation with 107 events in which both baryons go in the same direction, and 72 events in which they go in opposite direction.

This summer, data on $\Lambda\bar{\Lambda}$ correlations have become available from the TPC[18] and the MkII.[15] In the TPC there are 14 events with a pair of lambdas :

Λ-$\bar{\Lambda}$ = 11 *background* 1.4±1.2,
Λ-Λ = 3 *background* 2.1±0.9, and
$\bar{\Lambda}$-$\bar{\Lambda}$ = 0 *background* 0.6±0.7

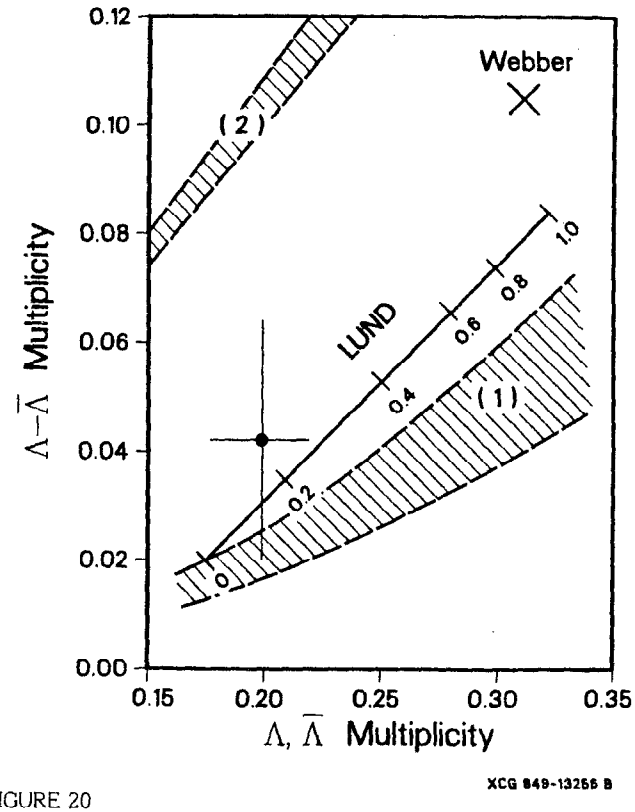

FIGURE 20

The Λ, $\overline{\Lambda}$ multiplicity and Λ-$\overline{\Lambda}$ pair multiplicity for the TPC data (+) compared to the LUND (solid line) and the Webber model (x). The upper band corresponds to predictions in which the Λ and $\overline{\Lambda}$ are maximally correlated and the lower band to predictions in which the Λ and $\overline{\Lambda}$ are minimally correlated See text for details.

i.e a minimum correlation.. The bands are bands rather than lines because they include a range of assumptions on the multiplicity distribution of baryons per event. The data point lies much closer to the assumption of minimum correlation. Figure 20 also shows the result of two model calculations. The Webber model predicts higher multiplicities of both Λ's and $\Lambda\overline{\Lambda}$ pairs in disagreement with the data even though it predicts the right multiplicity for π, K and p. This model, however, was not optimized to fit the Λ distributions. The LUND model can give a range of values depending on the value of the extra suppression factor for strange diquarks, $(us/ud)/(s/d)$, where (s/d) is the production ratio of strange and ordinary quarks from the vacuum and (us/ud) is the production ratio for strange and ordinary diquarks. A value $(us/ud)/(s/d)$ of $\simeq .2$ is in reasonable agreement with the data. Thus strange diquarks are suppressed by an additional factor of five when compared to the suppression for single strange quarks in the LUND model.

The above studies are clearly limited by statistics and will slowly improve in time as detectors collect more statistics and PEP increases its luminosity.

V. CONCLUSIONS

From the above progress report it is clear that the subject is complex and that definitive tests of models are difficult. Small differences in predictions do count and can reflect real problems with models as was shown in the analysis of particle flow in three jet events. A large amount of new data has been added during the last year: there are new areas for models to try to fit and many cross checks for experimental results. A lot remains to be done, but there is hope if the progress of last year is a clue to the future.

34. D. Blockus and B. Brabson, "*Comment About Our HRS rho/pi Ratio in e+e- Scattering*", informal comment submitted to this conference for this presentation.

35. R. Brandelik et al. (TASSO), Phys. Lett. 114B, 65 (1982); M. Althoff et al. (TASSO), Z. Physik. C22, 307 (1984).

36. H. Aihara et al. (TPC), Phys. Rev. Lett. 53, 130 (1984).

37. W. Bartel et al. (JADE), Phys. Lett. B134, 275, (1984).

38. A. Petersen , "*Further Studies on Quark and Gluon Fragmentations: Recent Results from Jade*," to appear in the Proceedings of the XV Symposium on Multiparticle Dynamics, Lund, Sweden, June 10-16, 1984.

39. H.Aihara et al. (TPC), "*Tests of Models of Parton Fragmentation Using 3-jet Events in e+e- Annihilation at* $\sqrt{s}$ *= 29 GeV*", LBL-18407, submitted for publication, October 1984.

40. H. Aihara et al. (TPC), "*Tests of Models for Quark and Gluon Fragmentation at* $\sqrt{s}$ *= 29 GeV*", LBL-18408, submitted for publication, October 1984.

41. E. Fernandez et al., "*A Measurement of Energy-Energy Correlations in e+e- to Hadrons at* $\sqrt{s}$ *= 29 GeV*", submitted to the XII International Conference on High Energy Physics, Leipzig, DDR, July 19-25, 1984.

42. H. Aihara et al. (TPC), "*Observation of Strangeness Correlations in e+e- Annihilation at* $\sqrt{s}$ *= 29 GeV*", LBL-18125, submitted to Phys. Rev. Lett.

43. R Brandelik et al.(TASSO), Phys. Rev. Lett. 100B, 357 (1981); Ch. Berger et al. (PLUTO), Nucl. Phys. 214B, 189 (1983).

44. D. Drijard et al., Nucl. Phys. 166B, 233 (1980).

45. M. Althoff et. al. (TASSO), Phys. Lett. 139B, 126 (1984).

46. K. Maruyama (TPC), "*Baryon Production in e+e-Annihilation at Vs = 29 GeV*", U. of Tokyo preprint UT-HE-84/09, to appear in the Proceedings of the Hadronic Sessions of the Nineteenth Recontre de Moriond, edited by J. Tran Thanh Van.